

The Different Flexibility of c-Src and c-Abl Kinases Regulates the Accessibility of a Druggable Inactive Conformation

Silvia Lovera,^{†,§} Ludovico Sutto,^{†,§} Ralitza Boubeva,[‡] Leonardo Scapozza,[‡] Nicole Dölker,^{*,†} and Francesco L. Gervasio^{*,†}

[†]Structural Biology and Biocomputing Programme, Spanish National Cancer Research Center (CNIO), Melchor Fernandez Almagro 3, E-28029 Madrid, Spain

[‡]Pharmaceutical Biochemistry, School of Pharmaceutical Sciences, University of Geneva, Quai Ernest-Ansermet 30, 1211 Genève 4, Switzerland

S Supporting Information

ABSTRACT: c-Src and c-Abl are two closely related protein kinases that constitute important anticancer targets. Despite their high sequence identity, they show different sensitivities to the anticancer drug imatinib, which binds specifically to a particular inactive conformation in which the Asp of the conserved DFG motif points outward (DFG-out). We have analyzed the DFG conformational transition of the two kinases using massive molecular dynamics simulations, free energy calculations, and isothermal titration calorimetry. On the basis of the reconstruction of the free energy surfaces for the DFG-in to DFG-out conformational changes of c-Src and c-Abl, we propose that the different flexibility of the two kinases results in a different stability of the DFG-out conformation and might be the main determinant of imatinib selectivity.

Protein kinases (PKs) are a large and functionally diverse protein family involved in cellular signaling and several vital biochemical functions.¹ Their deregulation is related to numerous human diseases, including inflammation, cardiovascular diseases, diabetes, and cancer, making them a fundamental target for drug design and development.² As all PKs catalyze the transfer of the γ -phosphate of ATP to a peptide substrate, it is not surprising that in the catalytically competent (active) state, they share a common fold with a structurally conserved catalytic pocket. This large structural homology complicates the quest for selective PK inhibitors. As inactive conformations are more structurally diverse in different kinases, inhibitors targeting inactive states are usually more selective.^{2a} One example of such an inhibitor is imatinib, which is used in the clinical treatment of chronic myeloid leukemia (CML) and other types of cancer.³ CML is caused by overactivation of the tyrosine kinase c-Abl due to the presence of the BCR-Abl fusion gene.⁴ Imatinib strongly inhibits c-Abl as well as the homologous PDGFR and c-KIT. However, it has a much lower inhibitory effect on the tyrosine kinase c-Src, although c-Src shares a higher (47%) sequence identity with c-Abl⁵ [Figure S12 in the Supporting Information (SI)] than PDGFR and c-KIT. Understanding the reasons underlying the selectivity of imatinib could provide crucial information for the rational design of new selective PK inhibitors.

The catalytic domain of PKs comprises an N-terminal lobe, containing mostly β -sheets, and a larger, α -helical C-terminal lobe⁶ (Figure 1). At the interface between the lobes, a number

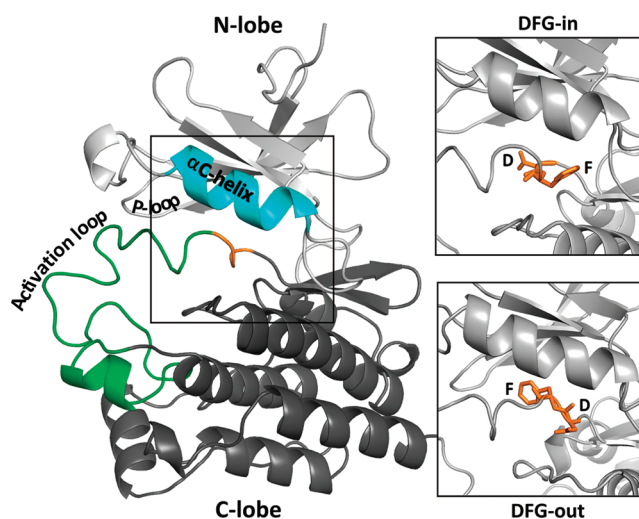


Figure 1. Structure of the kinase domain of c-Abl with a detailed view of the DFG motif in the DFG-in (upper inset, PDB entry 2G1T) and DFG-out (lower inset, PDB entry 1IEP) conformations.

of highly conserved residues form the active site with the ATP binding pocket. Kinase activation is mainly controlled by conformational changes in three conserved structural motifs at the active site: the activation loop (A-loop), the Asp-Phe-Gly (DFG) motif, and the α C-helix. The A-loop is a highly flexible region that can adopt an ensemble of different conformations ranging from an open form to a closed conformation, which completely blocks the substrate binding site. The α C-helix in the N-lobe can swing out of its active conformation (so-called α C-in), interrupting a crucial salt bridge in the active site and leading to a reoriented conformation (called α C-out).⁷ Finally, the DFG motif is located at the N-terminal end of the A-loop and has been proposed to have a role in the catalytic activity of the kinase.⁸ Crystal structures have shown that it can adopt at

Received: November 15, 2011

Published: January 23, 2012

least two distinct conformations (Figure 1 insets).^{8–10} In the DFG-in conformation, which can accommodate ATP, Asp404 (c-Src numeration) points toward the ATP binding site and Phe405 toward an adjacent hydrophobic pocket. In contrast, imatinib binds to a DFG-flipped conformation, called DFG-out, in which the Asp and Phe residues swap positions.

Initially, it was proposed that the low binding affinity of imatinib to c-Src was due to the inability of c-Src to adopt a DFG-out conformation.¹¹ However, recent crystal structures have shown that imatinib-bound conformations of c-Abl and c-Src are very similar.⁹ It has also been hypothesized that the DFG-out conformation has an important functional role and might be accessible to many if not most kinases.⁸ More recently, the differences in the inhibitory effect of imatinib on the two kinases have been ascribed to slight differences in the binding mode. Indeed, one of the N-lobe loops, the so-called P-loop, is known to adopt a distinct kinked conformation in the Abl–imatinib complex, while in c-Src it remains unchanged upon imatinib binding.¹⁰ The importance of the P-loop is further underlined by the fact that many mutations that confer resistance to imatinib are located in the P-loop.¹²

However, free energy calculations have shown that imatinib interactions with the DFG-out conformation are very similar in the two kinases.¹³ Thus, it is reasonable to hypothesize that intrinsic differences in the kinetics and thermodynamics of the conformational changes of the DFG motif itself play a significant role. Confirmation of this hypothesis would indicate that imatinib binds to PKs by a conformational selection mechanism.¹⁴ We studied this possibility by means of massive all-atom molecular dynamics (MD) simulations using both unbiased MD and an enhanced sampling method combining parallel tempering with well-tempered metadynamics (PTmetaD).¹⁵ We used PTmetaD to reconstruct the free energy surface of the conformational transition. Extensive sampling for more than 22 μ s allowed us to determine crucial differences between the DFG flips of c-Abl and c-Src. Our results show that the imatinib-bound conformation is both more accessible and more stable in c-Abl than in c-Src because of specific structural and dynamical features of the catalytic domain of c-Abl.

The starting structures were the catalytic domains of c-Src and c-Abl in the DFG-in conformation (PDB entries 2SRC and 2G1T, respectively) fully solvated in a box of water (see the SI). We used the very recent Amber99SB*-ILDN force field.¹⁶

Unbiased MD simulations lasting for 1000 ns revealed different patterns of flexibility in the DFG-in states of c-Src and c-Abl (Figure 2 and Figures S1 and S2). In particular, the α C-helix, the loops of the N-lobe, and the A-loop showed enhanced flexibility in c-Abl. Furthermore, there are differences in the dynamics of the residues of the hydrophobic pocket surrounding Phe405 (unless stated otherwise, the numbering of the amino acids refers to c-Src; see Figure 1). This is reflected most clearly in the distance between Phe405 and Leu317 (in c-Src) or Ile293 (in c-Abl). While in c-Src this distance fluctuates around a value of 4.6 ± 0.4 Å, in c-Abl two kinds of conformational transitions were observed, leading to a larger average distance of 5.2 ± 0.6 Å. Of the two, one involves a slight reorientation of the α C-helix and the other a flip of the side chain of Ile (Figure S3). The arrangement of the residues of the hydrophobic pocket is decisive for the stabilization of specific conformations of the DFG motif. Consequently, it could play a role in activation of the kinase domain.

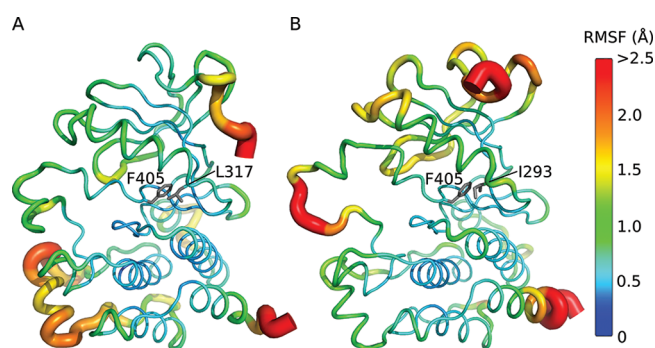


Figure 2. Equilibrated crystal structures in the DFG-in states of (A) c-Src and (B) c-Abl, colored according to root-mean-square fluctuations (RMSFs). The thickness of the tube is proportional to the RMSF.

To test whether there is a correlation between the flexibility of the N-lobe and the kinetics of activation of the catalytic domain, we reconstructed the free energy surfaces (FESs) for the DFG flips in the catalytic domains of c-Src and c-Abl by means of extensive PTmetaD calculations. In PTmetaD, different replicas of the system are run at different temperatures, and in each of them the potential is biased along one or more collective variables (CVs) that describe the conformational change under investigation. After extensive testing, we chose a range of 28 temperatures between 308 and 399 K and four different CVs (Figure S5).

Figure 3 shows the free energy as a function of the distances Asp404–Lys295 (CV1) and Phe405–Leu317/Ile293 (CV2) as

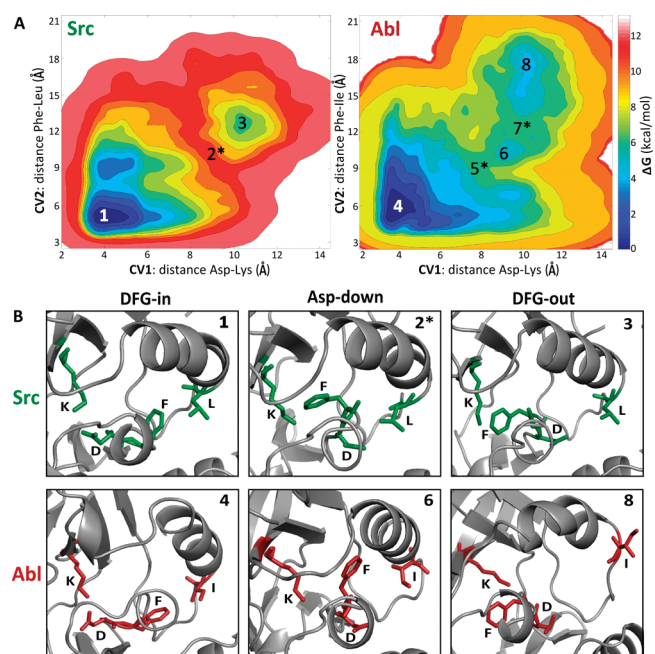


Figure 3. PTmetaD simulations of the kinase domains of c-Src and c-Abl. (A) Relative free energies of (left) c-Src and (right) c-Abl projected on the collective variables CV1 and CV2. The contour lines are drawn every 1 kcal/mol. (B) Structural details of the DFG motif and the α C-helix from representative structures for relevant minima and intermediates for c-Src (1, 2*, 3) and c-Abl (4, 6, 8).

well as close-ups of several relevant conformations. For both kinases, the global minimum of the FES, at low values for both CV1 and CV2, corresponds to the active DFG-in state (basins

labeled as 1 and 4 in Figure 3A for c-Src and c-Abl, respectively). In this state, Asp404 forms a salt bridge with Lys295 (CV1 \approx 4 Å) and Phe405 interacts with Leu317 (c-Src) or Ile293 (c-Abl) (CV2 \approx 5 Å). Both kinases also exhibit a pronounced local minimum at higher values of CV1 and CV2, which corresponds to the DFG-out state (basins 3 and 8 in Figure 3).

The free energy differences between the DFG-in and imatinib-binding DFG-out conformations (4.0 ± 0.5 kcal/mol for c-Abl and 6.0 ± 0.5 kcal/mol for c-Src) are large. These values might be overestimated as a result of systematic errors in the force field, but the value of $\Delta\Delta G$ would not be affected. At least in the case of c-Abl, protonation of Asp404 is expected to make the DFG-out state more accessible (see below).

The FESs reveal a number of crucial differences between the two systems. Both the free energy difference between the DFG-in and DFG-out states and the barrier separating the two states are noticeably lower for c-Abl than for c-Src. In c-Abl, the DFG-out state is 2 kcal/mol more stable than in c-Src, and the difference between the activation free energies for the DFG flips of c-Src and c-Abl amounts to 5 kcal/mol (Figure 3 and Figure S13). The imatinib-binding DFG-out conformation is therefore thermodynamically and kinetically favored in c-Abl relative to c-Src, a finding which is in agreement with the experimental observation that imatinib is a strong inhibitor for c-Abl but a very weak one for c-Src.⁹

Additionally, the FES of c-Abl reveals a third local minimum at CV1 = 9 Å and CV2 = 11 Å that lies 1 kcal/mol above the DFG-out state. This minimum, first observed in ref 8, corresponds to an intermediate conformation of the DFG flip transition in which the aspartate is pointing downward (Asp-down state; basin 6 in Figure 3). In contrast, the corresponding point on the FES of c-Src marks a transition state (state 2* in Figure 3). The Asp-down state in c-Abl is connected to the DFG-in and DFG-out states via two transition states (5* and 7*, respectively; Figure S4). Thus, the DFG flip in c-Abl takes place via a mechanism significantly altered from that in c-Src.

Previous calculations have shown that the contribution to the free energy difference of imatinib binding to c-Src and c-Abl is small ($\Delta\Delta G_{\text{bind}} = 0.2 \pm 0.6$ kcal/mol) for the kinases in their DFG-out conformations.¹³ Consequently, the experimentally measured differences in the overall binding affinities of imatinib should mainly be determined by the different relative stabilities of the DFG-out states.

The dissociation constant (K_D) for binding of imatinib to the unphosphorylated kinase domain of c-Abl has been determined with rather high precision by isothermal titration calorimetry (ITC) to be $K_D(\text{Abl}) = 0.08 \mu\text{M}$.⁹ However, the measurement of imatinib binding to c-Src is complicated by the low binding affinity and solubility of the drug; $K_D(\text{Src})$ values of $\sim 10 \mu\text{M}$ have been reported.^{9,17} We therefore carried out independent ITC measurements of $K_D(\text{Src})$ and performed western-blot and mass spectrometry analyses to confirm that the kinase was unphosphorylated (see the SI). We obtained the value $K_D(\text{Src}) = 7.2 \pm 2.2 \mu\text{M}$. This confirms that binding of imatinib to c-Src is very weak relative to binding to c-Abl. If it is assumed that the differences in imatinib binding to the DFG-out conformations of c-Src and c-Abl can be neglected, values of $K_D(\text{Abl}) = 0.08 \pm 0.05 \mu\text{M}$ ⁹ and $K_D(\text{Src}) = 7.2 \pm 2.2 \mu\text{M}$ would correspond to a difference of $\Delta\Delta G = 2.7 \pm 0.4$ kcal/mol in the relative free energies of the DFG-out states. The value of 2 ± 1 kcal/mol obtained from our extensive calculations is in good agreement with the experimental data, showing that the FESs of the DFG

flips can indeed explain the different sensitivities of c-Abl and c-Src toward imatinib and strengthening the case for a conformational selection binding mechanism.^{14a} However, conformational selection does not rule out a possible shift in the populations of the DFG-in state versus the DFG-out state due to interactions of imatinib with the binding site.¹⁸

The measured values for the dissociation constants K_D are, however, not in line with previously reported inhibition constants (K_i) for inhibition of the enzymatic activity of c-Abl and c-Src kinase domains by imatinib [$K_i(\text{Abl}) = 0.013 \mu\text{M}$ and $K_i(\text{Src}) = 44.9 \pm 7.6 \mu\text{M}$].⁹ An explanation for this disagreement most probably lies in the different experimental conditions for the K_i and ITC measurements.

The analysis of the specific features of the two FESs can explain the different propensities for the DFG-out state. One distinctive mark of the FES of c-Abl is that all of the local minima, but particularly the one corresponding to the DFG-out state, are significantly wider than in the case of c-Src, indicating enhanced flexibility of c-Abl. Furthermore, while the values of CV1 in the minima of the DFG-out states are similar for the two systems, the values of CV2 differ. For c-Abl, the minimum is shifted to larger Phe–Ile distances. Structural analysis shows that this is due to changes in the conformation and orientation of the αC -helix (Figure 3C). In c-Abl, the αC -helix becomes distorted, and the side chain of Ile293 shows a higher mobility and a tendency to shift away from the hydrophobic pocket. At the same time, the upward movement of the αC -helix widens the active site.

Generally, the entire N-lobe of c-Abl, and particularly its solvent-exposed loops, seem to show enhanced flexibility relative to c-Src. To quantify the different flexibilities, we projected the FESs of the DFG flips onto four new CVs describing the relative orientation of the loops and the distance between the αC -helix and the more rigid C-lobe (see Computational Methods in the SI and Figure S9A).

All of the projections of the FESs of c-Src and c-Abl along these new CVs show the same trends. While in the case of c-Src there is generally only one steep minimum, showing that no conformational changes of the N-lobe occur during the simulation, for c-Abl there are either various minima or a very broad one (Figure S9B). This analysis confirms that in c-Abl the N-lobe exhibits pronounced flexibility, allowing conformational changes of the P-loop, the $\beta 4$ – $\beta 5$ loop, the $\beta 3$ – αC loop preceding the αC -helix, and the αC -helix itself. The enhanced flexibility allows the αC -helix to adopt conformations not accessible for c-Src. In c-Abl, the P-loop assumes different conformations even in the absence of inhibitors. The changes in the P-loop are transmitted to the catalytically important αC -helix via the $\beta 3$ – αC loop. It is tempting to speculate that the resulting distortion of the αC -helix leads to an interruption of the hydrophobic cluster at the interface of the two lobes,¹⁹ weakening its interactions with Phe405. As a result, the DFG-in state in c-Abl would be destabilized and the activation barrier for the DFG flip lowered, and the DFG-out state, in which the polar Asp404 points toward the partially disrupted hydrophobic cluster, would become more favorable.

Furthermore, the widening of the active site in the DFG-out state of c-Abl due to the shift and distortion of the αC -helix may allow the entrance of additional water molecules into the active site. To test this hypothesis, we calculated the solvent-accessible surface areas (SASs) of the active sites for the DFG-in and DFG-out states (see the SI). In the DFG-in state, the active-site SASs are $5900 \pm 200 \text{ Å}^2$ in c-Src and $6000 \pm 100 \text{ Å}^2$

in c-Abl. In the DFG-out state, the active site in c-Src remains unaffected by the DFG flip ($SAS = 5900 \pm 100 \text{ \AA}^2$) while in c-Abl the average size of the cavity increases to $6200 \pm 200 \text{ \AA}^2$.

The enlargement of the active site in c-Abl increases the amount of water found in the vicinity of the DFG motif. While in c-Src the average number of water molecules within 5 Å of the residues of the DFG motif is 19 ± 3 in both the DFG-in and DFG-out states, in c-Abl it increases from 19 ± 5 in the DFG-in state to 22 ± 5 in the DFG-out conformation. The entrance of up to three additional water molecules into the cavity, which could stabilize Asp404 through H-bond formation, may very well contribute significantly to the stabilization of the DFG-out state.

It has been proposed that protonation of Asp404 of the DFG motif should affect the DFG-flip propensity in the Abl kinase.⁸ Consequently, it is conceivable that protonation could also alter the free energy differences between c-Abl and c-Src. To test this possibility, we estimated the pK_a values for c-Src and c-Abl in the DFG-in and DFG-out states (see the SI). For c-Src, we obtained a Asp404 pK_a values of 4.0 ± 0.5 in the DFG-in state and 2.6 ± 0.3 in the DFG-out state. For c-Abl, $pK_a = 3.4 \pm 0.5$ and 4.4 ± 0.4 in the DFG-in and DFG-out states, respectively (Figure S10). These results indicate that in the case of c-Abl, protonation of Asp404 would indeed stabilize the DFG-out state by 1.4 ± 0.9 kcal/mol, while in c-Src, the DFG-out conformation would become even less favorable (by 2.0 ± 0.9 kcal/mol). In any event, the low pK_a value indicates that protonation of Asp404 in c-Src in the DFG-out state is improbable. We also addressed the influence of the protonation of Asp404 on the distance between Phe405 and Leu317 in c-Src. To this end, we carried out metadynamics simulations of protonated and unprotonated c-Src in the most favorable DFG-in conformation using the Phe405–Leu317 distance and the χ_1 angle of Phe405 as CVs (see the SI). Comparison of the two FESs revealed that protonation of Asp404 has no influence on the local dynamics of Phe405 in c-Src (Figure S11).

To summarize, by performing massive free energy calculations, we have found important differences in the energetics of the conformational change of the DFG motif in c-Abl and c-Src, which is known to be involved in the catalytic process as well as in binding to the anticancer drug imatinib. On the basis of a comparison between ITC measurements of the binding affinities of imatinib and the calculated free energies of the DFG flip, we propose that the dissimilar inhibitory effects of imatinib on the two kinases is mainly due to the better accessibility of the DFG-out conformation in c-Abl and that a ligand binding to this particular state selects rather than induces it. We have shown that these differences can be attributed mainly to the greater flexibility of c-Abl. The differential flexibility affects not only the energetics of the DFG flip but also the conformation of the N-lobe loops. As these characteristics arise from structural features that are far from the active site, they could be used to develop a new class of allosteric Abl inhibitors.

■ ASSOCIATED CONTENT

■ Supporting Information

Computational and experimental methods, additional results, complete refs 8 and 17, and movies (MPG) showing the DFG flip. This material is available free of charge via the Internet at <http://pubs.acs.org>.

■ AUTHOR INFORMATION

Corresponding Author

andolker@cnio.es; flgervasio@cnio.es

Author Contributions

[§]These authors contributed equally.

Notes

The authors declare no competing financial interest.

■ ACKNOWLEDGMENTS

We acknowledge the Ministerio de Ciencia e Innovación and CAM (Grants BIO2010-20166 and BIPEDD2) and DEISA and the BSC for computer time. L.S. and S.L. acknowledge support by a Juan de la Cierva Research Fellowship and an FPI Grant, respectively, from MICINN. We thank Prof. John Kuriyan (University of California Berkeley) for providing the YopH phosphatase plasmids and Drs. R. Perozzo, G. Saladino, and S. Marsili for fruitful discussions.

■ REFERENCES

- (1) Manning, G.; Whyte, D.; Martinez, R.; Hunter, T.; Sudarsanam, S. *Science* **2002**, 298, 1912.
- (2) (a) Noble, M. E. M.; Endicott, J. A.; Johnson, L. N. *Science* **2004**, 303, 1800. (b) Matthews, D. J.; Gerritsen, M. E. *Targeting Protein Kinases for Cancer Therapy*; Wiley: Hoboken, NJ, 2011.
- (3) Capdeville, R.; Buchdunger, E.; Zimmermann, J.; Matter, A. *Nat. Rev. Drug Discovery* **2002**, 1, 493.
- (4) (a) Hantschel, O.; Superti-Furga, G. *Nat. Rev. Mol. Cell. Biol.* **2004**, 5, 33. (b) Daley, G. Q.; van Etten, R. A.; Baltimore, D. *Science* **1990**, 247, 824.
- (5) Deininger, M.; Buchdunger, E.; Druker, B. J. *Blood* **2005**, 105, 2640.
- (6) (a) Knighton, D.; Zheng, J.; ten Eyck, L.; Ashford, V. *Science* **1991**, 253, 407. (b) Lowe, E. D.; Noble, M. E.; Skamnaki, V. T.; Oikonomakos, N. G.; Owen, D. J.; Johnson, L. N. *EMBO J.* **1997**, 16, 6646.
- (7) Xu, W.; Doshi, A.; Lei, M.; Eck, M.; Harrison, S. *Mol. Cell* **1999**, 3, 629.
- (8) Shan, Y.; et al. *Proc. Natl. Acad. Sci. U.S.A.* **2009**, 106, 139.
- (9) Seeliger, M. A.; Nagar, B.; Frank, F.; Cao, X.; Henderson, M. N.; Kuriyan, J. *Structure* **2007**, 15, 299.
- (10) Seeliger, M. A.; Ranjitkar, P.; Kasap, C.; Shan, Y.; Shaw, D. E.; Shah, N. P.; Kuriyan, J.; Maly, D. J. *Cancer Res.* **2009**, 69, 2384.
- (11) (a) Druker, B.; Tamura, S.; Buchdunger, E.; Ohno, S. *Nat. Med.* **1996**, 561. (b) Schindler, T.; Bornmann, W.; Pellicena, P.; Miller, W.; Clarkson, B.; Kuriyan, J. *Science* **2000**, 289, 1938.
- (12) Shah, N. P.; Nicoll, J. M.; Nagar, B.; Gorre, M. E.; Paquette, R. L.; Kuriyan, J.; Sawyers, C. L. *Cancer Cell* **2002**, 2, 117.
- (13) Aleksandrov, A.; Simonson, T. J. *Biol. Chem.* **2010**, 285, 13807.
- (14) (a) Tsai, C. J.; Ma, B.; Nussinov, R. *Proc. Natl. Acad. Sci. U.S.A.* **1999**, 96, 9970. (b) Boehr, D. D.; Nussinov, R.; Wright, P. E. *Nat. Chem. Biol.* **2009**, 5, 789.
- (15) Bussi, G.; Gervasio, F. L.; Laio, A.; Parrinello, M. *J. Am. Chem. Soc.* **2006**, 128, 13425.
- (16) Piana, S.; Lindorff-Larsen, K.; Shaw, D. E. *Biophys. J.* **2011**, 100, L47.
- (17) Karaman, M. W.; et al. *Nat. Biotechnol.* **2008**, 26, 127.
- (18) D'Abramo, M.; Rabal, O.; Oyarzabal, J.; Gervasio, F. L. *Angew. Chem., Int. Ed.* **2012**, 51, 642.
- (19) Kornev, A. P.; Haste, N. M.; Taylor, S. S.; Eyck, L. F. T. *Proc. Natl. Acad. Sci. U.S.A.* **2006**, 103, 17783.